**Atmospheric
Chemistry
and Physics
Discussions**

Statistical analysis of non-methane hydrocarbon variability at a European background location (Jungfraujoch, Switzerland)

V. A. Lanz[1,*], C. Hueglin[1], M. K. Vollmer[1], M. Steinbacher[1], S. Henne[1],
J. Staehelin[2], B. Buchmann[1], and S. Reimann[1]

[1]Empa, Swiss Federal Laboratories for Materials Testing and Research, Laboratory for Air Pollution and Environmental Technology, 8600 Duebendorf, Switzerland
[2]Institute for Atmospheric and Climate Science, ETH Zurich, 8092 Zurich, Switzerland
[*]now at: PSI (Paul Scherrer Institute) Laboratory for Atmospheric Chemistry, 5232 Villingen PSI, Switzerland

Correspondence to: V. A. Lanz (lanzv@ethz.ch)

Title Page

Abstract	Introduction
Conclusions	References
Tables	Figures

|◄ | ►|
◄ | ►

Back | Close

Full Screen / Esc

Printer-friendly Version

Interactive Discussion

Abstract

In-situ measurements of volatile hydrocarbons, C_xH_y, and chlorinated organic compounds, $C_xH_yCl_z$, were performed at Jungfraujoch (Switzerland) during eight years (2000–2007). The analysis of 4-hourly resolved non-methane hydrocarbons (NMHCs)

5 was achieved by using gas-chromatography coupled with mass spectrometry (GC-MS). Variabilities in the NMHC series were modeled by factor analysis. Four factors defined the solution space and could be related to hydrocarbon sources. In order to facilitate factor interpretations the retrieved contributions were compared with independent measurements, such as trace gases (NO_x, CO, and CH_4) and meteorological data

10 (back trajectories). The most dominant factor (accounting on average for 42% of the total mixing ratio of the considered NMHCs) was found to be most active in winter, covarying with CO and could be related to combustion sources. The other three factors represent both industrial and evaporative sources. Trajectory statistics suggest that the most influential anthropogenic NMHCs sources for Jungfraujoch are located in Eastern

15 Europe, but the Po Valley has been identified as a potential source region for specific industrial sources as well. Aging of the arriving NMHCs, the derived factors as well as limitations of the methods are discussed.

1 Introduction

Measurements of the composition of trace gases at mountain sites, such as the high-

20 alpine observatory at the Jungfraujoch located at 3580 m a.s.l. in Switzerland, offer unique possibilities because the site is intermittently exposed to air advected from the polluted planetary boundary layer or from the clean lowermost free troposphere. The latter properties have been used to study the chemistry of the free troposphere (e.g., Zanis et al., 2003, 2007; Walker et al., 2006; Cozic et al., 2008; Parker et al., 2008[1]) as

---

[1]Parker, A. E., Monks, P. S., Wyche, K. P., Balzani-Lööv, J. M., Staehelin, J., Reimann, S., Legreid, G., Vollmer, M. K., and Steinbacher, M.: Peroxy radicals in the summer free tropo-

well as long-term changes of background mixing ratios of trace gases (Reimann et al., 2005, 2008) and tropospheric ozone (Ordoñez et al., 2007). Jungfraujoch is therefore a suitable site for background measurements as performed within the Global Atmosphere Watch (GAW) programme of the World Meteorological Organization (WMO) and projects like SOGE (System for observation of halogenated greenhouse gases in Europe). Measurements at Jungfraujoch also provide valuable information to study trace gases as well as aerosols emitted into the planetary boundary layer (e.g. Lugauer et al., 1998). In all such analyses air advected from the planetary boundary layer and air from the free troposphere need to be distinguished. This distinction was performed by different methods using chemical tracers (e.g. Carpenter et al., 2000; Zellweger et al., 2003), meteorological indicators (e.g. Forrer et al., 2000; Henne et al., 2005), or combinations of both (Henne et al., 2008a). Another method is based on the analysis of backward trajectories of air masses arriving at Jungfraujoch and identification whether or not they were in contact with the planetary boundary layer (e.g., Legreid et al., 2008). When dealing with the composition of trace gases sampled at high mountain sites the changes due to atmospheric oxidation during transport need to be considered as well (Li et al., 2005).

In this study, factor analysis (Seber, 1984; Krzanowski, 1988) was applied to organic trace gas measurements at Jungfraujoch. This method explains the variability of trace gas concentrations by a few underlying factors. No prior assumptions, such as meteorological conditions prevailing at the measurement site, is required for this application. Several studies have applied factor analysis and similar multivariate methods to determine emission sources that have an impact on air pollution at selected receptor sites. For example, uncertainty-weighted and positively constraint factor analysis (PMF2; Paatero, 1997) was successfully used to characterize particulate and gaseous emission sources in the planetary boundary layer of an urban background site in Zurich,

sphere: seasonality and heterogeneous loss, Atmos. Chem. Phys. Discuss., 8, 17 841–17 889, 2008,
http://www.atmos-chem-phys-discuss.net/8/17841/2008/.

Title Page

Abstract | Introduction

Conclusions | References

Tables | Figures

◄ | ►

◄ | ►

Back | Close

Full Screen / Esc

Printer-friendly Version

Interactive Discussion

Switzerland (Lanz et al., 2007, 2008a).

The aim of the present study is to investigate factors driving NMHC variability at Jungfraujoch during the past eight years (2000–2007). The PMF2 obtained factors for the NMHCs at Jungfraujoch though can not be expected to depict fresh emission profiles reported in the literature as aging of the air masses covers the source tracks of airborne organics. This study further evaluates the capability of factor analysis when applied to reactive substances retrieved from remote measurement sites. After the description of the measurements and the applied factor analysis the determined factors are interpreted by making use of simultaneous inorganic air pollutant measurements (nitrogen oxides, NO and NO_2, carbon monoxide, CO), methane (CH_4) and backward trajectory analysis providing information on potential locations of anthropogenic NMHC emission sources.

2   Methods

2.1   Measurements

2.1.1   NMHC measurements

The high altitude research station Jungfraujoch ($7°\,59'$ E, $46°\,32'$ N, 3580 m a.s.l.) is situated on a mountain saddle in the central Swiss Alps between the Jungfrau mountain (4158 m a.s.l.) in the West and the Mönch mountain (4099 m a.s.l.) in the East. Due to its high elevation, its central location in Europe, the proximity to source regions of anthropogenic greenhouse gases measurements at Jungfraujoch can capture both advected air from the polluted boundary layer as well as air from the lower free troposphere (European background). The time span in this study includes eight years of measurement (1 January 2000 to 31 December 2007).

Measurements of NMHCs are conducted using a fully automated gas-chromatograph (GC) mass-spectrometry (MS) (Agilent 6890 and 5793N) system with

a custom-built preconcentration unit (adsorption-desorption system ADS; Simmonds et al., 1995) to allow for sample trapping of 2 L of air for each measurement. The trace gases are collected on a microtrap at −50°C for 40 min and thermally desorbed at ∼240°C before they are chromatographically separated on a 120 m×0.32 mm I.D. CP-SIL 5CB capillary column (Chrompack) with 5 μm film thickness, and detected using single-ion mode quadrupole mass spectrometry.

Air sample measurement runs are completed after 2 h each and are bracketed by working standard measurements to determine and correct for instrumental drift, resulting in usually six ambient air observations per day. These working standards are prepared by compressing ambient air into 35 L electropolished stainless steel canisters (Essex Cryogenics, Missouri, USA), by means of a modified oil-free compressor (model SA-3, RIX, California, USA). These working standards are referenced against hydrocarbon standards (National Physical Laboratories, Teddington, UK) and against transfer standards relating the chlorinated NMHC measurements to the University of Bristol-98 (for dichloromethane and trichloroethene) and the NOAA-2003 (for tetrachloroethene) calibration scales. The mean precisions (1σ) of the Jungfraujoch NMHC measurements are <2 % as determined from the precision of the working standard measurements. The accuracies of the results are estimated at <10 %.

The species used in this study are summarized in Table 1. NMHCs with an atmospheric lifetime between 2 days and 0.5 year were selected.

2.1.2 Ancillary data

Continuous long-term in-situ measurements of a comprehensive set of other trace gases at Jungfraujoch are conducted as part of the Swiss National Air Pollution Monitoring Network (NABEL) that is operated by Empa in joint collaboration with the Swiss Federal Office for the Environment (FOEN). Carbon monoxide (CO) is monitored via non-dispersive infrared-absorption (APMA 360; Horiba Instruments Ltd) and NO$_x$ was measured with chemiluminescence detectors (Cranox, CLD 770 AL ppt, Ecophysics) (Zellweger et al., 2000). Methane (CH$_4$) is determined since 2005 by GC with flame ion-

ization detection (GC-FID) (Agilent 6890N) and detailed by Steinbacher et al., (2008)[2].

2.2 Data analysis

2.2.1 Matrix factorization

For bilinear mixing models it is assumed that an observed concentration or mixing ratio, x_{ij}, can be linearly approximated by p sums of products, $g_{ik}f_{kj}$, up to some error, e_{ij}:

$$x_{ij} = \sum_k g_{ik}\, f_{kj} + e_{ij},\, i=1\ldots m,\, j=1\ldots n,\, k=1\ldots p, \tag{1}$$

where f_{kj} represents the jth species loading in the kth factor and g_{ik} the score of the kth factor in the ith sample. Both g_{ik} and f_{kj} are estimated in this approach. The model equation above can be rewritten in matrix notation as follows

$$\mathbf{X} = \mathbf{GF} + \mathbf{E}, \tag{2}$$

where $\mathbf{G}$ is an $n{\times}p$-matrix containing p factor scores or contributions over n samples in time and $\mathbf{F}$ is an $p{\times}m$-matrix representing p factor profiles including m measured quantities. Paatero and Tapper (1993, 1994) showed that principal component analysis (PCA) as a least-square fit to the data matrix elements x_{ij} might be badly weighted and proposed heteroscedastic errors for their model (positive matrix factorization, PMF). Uncertainty values, σ_{ij} (based on the measurement error), are estimated for each data point, x_{ij}, and are used to weight ($w_{ij}=\sigma_{ij}^{-1}$) the residuals, e_{ij} (see Eq. 1), in the chi-square metric:

$$Q = \sum_i \sum_j (e_{ij}w_{ij})^2, \tag{3}$$

---

[2]Steinbacher, M., Vollmer, M. K., Brunner, D., Henne, S., and Reimann, S.: Quasi-continuous CH_4, N_2O, and SF_6 measurements at the high Alpine site Jungfraujoch (3580 m a.s.l.): influence of transport processes and emissions estimates, in prep.

where Q is to be minimized with respect to both g_{ik} and f_{kj}. The program PMF2 written by Paatero (1997) was designed to solve this task restricting the solution to non-negative values only, which allow for a quantitative interpretation of the factors. The model parameters and uncertainty estimates were specified as described for chromatographic data (GC-FID) elsewhere (Lanz et al., 2008a).

2.2.2 Data projections

Henry (1997, 2003) has used a geometrical approach to visualize the receptor problem (Eqs. 1 and 2) and to derive starting values for his bilinear unmixing algorithm (UNMIX). It is based on the assumption that there are samples in the data representing pure (or absent) sources. As we measured distant to anthropogenic NMHC sources, the factor profiles **F** can not be directly related to emission profiles. In order to check the connection of the PMF-solution with the physical reality we projected the PMF-resolved profiles along with the real NMHC-samples onto the planes spanned by standardized principal components (PCs) as described below.

First, the observables j were divided by their median, $\tilde{\mathbf{X}} : =\mathbf{X}_{ij}/median(\mathbf{x}_j)$, to make their scales comparable (normalization). Then, the PCs of the matrix $\tilde{\mathbf{X}}_{ij}$ (rank $p<m$), which equal $\mathbf{U}\boldsymbol{\Lambda}$), were determined by singular value decomposition (SVD; described in more detail in Golub and Van Loan, 1996):

$$\tilde{\mathbf{X}}=\mathbf{U}\,\boldsymbol{\Lambda}\,\mathbf{V}^t, \tag{4}$$

where **U** is an $n \times m$-matrix, $\boldsymbol{\Lambda}$ and **V** transposed are both orthogonal $m \times m$-matrices. The matrix-product $\mathbf{U}\boldsymbol{\Lambda}$ contains the principal component scores, which are the coordinates of the sources in the space of the principal components. All but the first p diagonal elements in $\boldsymbol{\Lambda}$ were set to 0 to obtain $\boldsymbol{\Lambda}_p$ and the standardized scores were calculated as

$$\mathbf{G}^{std}=\mathbf{U}\boldsymbol{\Lambda}_p/(\mathbf{u}_j\lambda_{p=1}), \tag{5}$$

ACPD

8, 19527–19559, 2008

Factor analysis of remote NMHCs

V. A. Lanz et al.

Title Page

Abstract | Introduction

Conclusions | References

Tables | Figures

◄ | ►

◄ | ►

Back | Close

Full Screen / Esc

Printer-friendly Version

Interactive Discussion

Here, p represents the reduced dimensions of the data in $\mathbb{R}^m$, the m-dimensional subspace. The simplex spanned by the p factors is called solution space. The standardization given in Eq. 5 reduces the dimensionality of the PC coordinate system to $p - 1$. These projections also allow to check the dimensionality p as specified within the PMF analysis.

2.2.3 Trajectory statistics

For the years 2002–2007, backward air mass trajectories are available for Jungfraujoch (48 hrs back in time, 6 trajectories per day, initial altitude at ∼100 m above model ground). These trajectories were computed using the model TRAJEC (Fay et al., 1995) and are based on hourly 3-dimensional wind fields (7 km×7 km horizontal resolution and 45 vertical levels) from the COSMO model. COSMO is an operational numerical weather prediction model (Consortium for Small-scale Modeling, http://cosmo-model.cscs.ch/) of MeteoSwiss (Federal Office of Meteorology and Climatology). The resulting trajectories were loaded with the PMF calculated factor contributions, g_{ik}, and the corresponding mixing ratios were redistributed within the European domain. A grid was superimposed to the domain of the COSMO trajectories. Initially, a mean mixing ratio was calculated for each grid cell according to Seibert et al. (1994). Then, a residence time- and trajectory segment-weighted mean was used to recalculate the distribution of the mixing ratio field as proposed by Stohl (1996):

$$\overline{g}_{k,ab} = (\sum_l \sum_h \tau_{abhl})^{-1} \sum_l \sum_h \log(g_{k,hl}) \tau_{abhl}, \tag{6}$$

where τ_{abhl} represents the residence time of segment h of trajectory l in grid cell (a,b) and $g_{k,hl}$ is the initially redistributed contribution of the kth factor.

The results are shown for grid cells hit (i.e., when the trajectory was below a seasonally variable boundary layer height, defined by a pressure difference of ∼200 hPa above model ground) by at least 10 trajectories. This procedure can not be expected

to be quantitative, but gives an indication for potential source regions of the considered pollutants (more details can be found in Reimann et al., 2004). We assume that the typical transport time from source to receptor is 2 days or less, which is shorter than the atmospheric lifetime of toluene (~2.4 d), the most reactive substance studied here
5 (see Table 1).

3 Results and discussion

3.1 Dimensionality and visualization of the PMF-solution

The determination of the number of factors is not closing for all techniques of dimensionality reduction and receptor models. This holds even more for data collected at
10 remote sites, where the calculated receptor profiles can not be directly related to fresh emission profiles reported in the literature.

We chose four factors (p=4, Eq. 1) to approximate the full data matrix. This solution yields a Q-value (see Eq. 3) of ~10^5, which is in line with what is expected for an nm-element data matrix (m=10, n~10000). This means that overall the assumed
15 uncertainties $\mathbf{S}$ approximate the model error $\mathbf{E}$, $\mathbf{S}{\approx}\mathbf{E}$. This criterion is essentially a mathematical one and does not guarantee that the PMF-solution can be related to physical reality.

In addition, the four factor profiles as calculated with the PMF2 program were appended to the data matrix $\mathbf{X}$ and subject to the data projection as described above
20 (Eqs. 4 and 5). Figure 1 shows the NMHC measurements projected onto the standardized PC planes along with the 4-factorial PMF solution. The PMF-modeled profiles lie close to the vertices of the facets (defined by $\mathbf{G}^{\text{std}}$) in the coordinate system of the standardized PC scores. Therefore, the PMF-solution seems connected with the physical reality, which also clearly reduces its potential rotational uncertainty. From these
25 projections, it can easily be deduced that the PMF-solutions are very close to the vertices of a tetrahedron (i.e. a 3-dimensional simplex defined by the data), supporting

the choice of a 4-factorial solution in this application. Additionally, the choice of more factors, $p=5, 6, 7, \ldots$, results in unrealistic factor profiles representing single species (see Sect. 3.2). In Fig. 1 (top panel) a few samples lie beyond factor 3 (i.e., higher PC2 and lower PC1 scores) allegedly providing a better solution profile. However, these samples exhibit an overwhelming toluene peak and Li et al. (2005) have hypothesized that a local source might cause such events. As indicated by this plot (Fig. 1, top panel), these toluene dominated samples were down-weighted in the robust mode of the PMF2 algorithm and do not determine the shape of factor 3 (Fig. 2).

The benzene:toluene ratio (as shown for the standardized PC1 scores vs. PC2 scores in Fig. 1, top panel) has been used to calculate a "photochemical age" of the air masses at receptor sites by assuming common sources and constant emission ratios for the two compounds (Roberts et al., 1984). However, as pointed out by McKeen and Liu (1993) this idealistic concept overrides non-linear processes that influence the benzene:toluene ratio in non-isolated air parcels from source to receptor, such as uptake of fresh emissions on the transport path and mixing with background air of variable composition. Therefore, NMHC ratios can not be expected to provide an accurate absolute age of the arriving air masses, but may serve as a qualitative indication of the age/origin of the air masses. Li et al. (2005) and Lanz et al. (2008c)[3] showed that the benzene:toluene ratio can be indicative for the photochemical age of the arriving air masses at Jungfraujoch, at least for selected periods. The top panel in Fig. 1 indicates that factor 1 (aged air masses) and factor 3 (fresh emissions) span the full range of air mass ages observable at Jungfraujoch during 2000–2007. This is pointing to the possibility that these factors are not only indicative for emission sources, but also for atmospheric processes, such as aging of air masses.

A stratification of the samples can also be described by factors 2 and 4 with respect to the trichloroethene:dichloromethane ratio (Fig. 1, middle panel) as well as the trichloro-

---

[3]Lanz, V. A., Hueglin, C., and Prévôt, A. S. H.: Transport and ageing of organic aerosols, Geophysical Research Abstracts, 10, EGU2008-A-06928, 2008c. www.cosis.net/abstracts/EGU2008/06928/EGU2008-A-06928-1.pdf?PHPSESSID=

Printer-friendly Version

Interactive Discussion

methane:benzene ratio (Fig. 1, lower panel). While the substances of the former ratio have different lifetimes, those of the latter are very similar (Table 1) further questioning the conclusiveness of NMHC ratios as surrogates for air mass clocks.

In addition, it should be noted that the sources of benzene and toluene are not identical - the extreme benzene:toluene ratios might simply indicate that factors 1 and 3 represent compositional changes with this respect. This seems plausible as wood burning emissions for instance were characterized by a benzene:toluene ratio of 10, whereas a ratio of 0.5 or less was estimated for fossil fuel burning (Lanz et al., 2008a). Recent research suggests that wood burning is a seasonally important source of airborne organics in Europe, e.g. in Helsinki (Saarikoski et al., 2008), in Zurich (Lanz et al., 2008b) or in the Alps (Sandradewi et al., 2008; Gaeggeler et al., 2008). On the other hand, many solvents contain toluene but virtually no benzene, yielding a benzene:toluene ratio of ∼0.

3.2 Factor profiles

The factor profiles are discussed in terms of explained variability, EV,

$$EV_{kj} := \sum_i |g_{ik}f_{kj}| / (\sum_i (\sum_h |g_{ih}f_{hj}| + |e_{ij}|)), \tag{7}$$

the relative contribution of each factor k to the individual compounds j, as their absolute mixing ratios in ambient air are on different scales and not directly comparable.

Factor 1 explains the variability of combustion-related C_4 and C_5 hydrocarbons (isobutane (56%), butane (65%), pentane (45%), isopentane (30%) and hexane (45%) as well as benzene (46%)). Virtually no chlorinated NMHCs are included in this factor. Benzene mixing ratios are over-represented as opposed to fresh emission profiles of both wood and fossil fuel combustion (Lanz et al., 2008a). Benzene is the longest-lived hydrocarbon considered here and, for this reason, factor 1 is interpreted as a (highly) aged combustion profile (for an overview of tentative factor interpretations see Table 3).

Factor analysis of remote NMHCs

V. A. Lanz et al.

Factor 3 also explains the variability of mainly hydrocarbon species. But in contrast to the first factor, compounds that can be associated with industrial solvent-use or evaporation, such as iso-pentane (35%), pentane (32%), hexane (31%) and toluene (70%) are included in factor 3. The hydrocarbon profile is very similar (R^2=0.99, n=7)
5 to the profile "solvent use" estimated for urban data (Lanz et al., 2008a).

The chlorinated compounds are predominantly distributed to factors 2 and 4. Factor 2 comprises the long-lived dichloromethane (70%) and tetrachloroethene (56%). Hydrocarbons play a minor role (and possibly represent mixing with background air): benzene (37%), isobutane (29%) etc. The fourth factor explains most of the trichloro-
10 ethene variability (92%), and to some minor extent also tetrachloroethene (20%) and dichloromethane (12%).

Only between 3% (trichloroethene) and 24% (hexane) of the variabilities remain unexplained by the model. Increasing the number of factors to p=5 leads to a factor that almost exclusively explains hexane variability ($EV_{5,\text{hexane}}$=96%). Assuming even more
15 factors yields additional factors that predominantly explain the variability of individual compounds. This can be explained by the fact that the long-term background variability of individual compounds makes up about half of the computed Q (see Eq. 3). For this calculation, baseline values for each NMHC species were estimated in analogy to Novelli et al. (1998) and Thoning et al. (1989), subtracted from the NMHC measurement
20 series, and PMF2 was re-run for these background corrected data (the background mixing ratios of each species were approximated by a polynomial quadratic equation and the window width of the low-pass filter was set to 80 days). This analysis further revealed that the differences between the factor profiles calculated for background corrected and uncorrected data are negligible when p=4 (or less) factors were prescribed.

3.3 Factor contributions

3.4 Seasonality

The factor contributions, $\mathbf{g}_{ik}$ (time series in ppb), are shown in Fig. 3. Monthly boxplots were calculated to represent the seasonally different cycles of the four factors (Fig. 4). While factor 1 is active in winter, factor 2 exhibits the highest mixing ratios in the warm season. On the other hand, factor 3 and factor 4 do not show an explicit seasonal cycle for their absolute contributions in ppb (but show summer maxima when their relative contributions in % ppb/ppb are considered). As shown in Fig. 2 most NMHCs included in the statistical analysis are represented by different factors, e.g. the isobutane mixing ratio makes up a substantial fraction of factor 1-profile (∼25%), but also in the profile of factor 2 (∼15%) and a minor fraction in factor 4 (∼5%). Therefore, the classification by PMF allows for further information about NMHC variability that is not evident from separate analyses of single compounds, as all measured hydrocarbons (except toluene) show a yearly cycle with maxima in winter (Fig. 4, lower left panel).

This hydrocarbon accumulation in winter can be observed at several remote sites in the Northern hemisphere, e.g. in Canada (Bottenheim and Shepherd, 1995) or Germany (Klemp et al., 1997), representing one potential driver of spring maxima of ozone (Monks, 2000). This accumulation may be in part caused by the seasonal variation of hydroxyl radical concentrations [HO˙], but also due to more medium-range transport from polluted areas to remote locations in wintertime. Toluene, on the other hand, does not show a distinct seasonal variation (Fig. 4, lower right panel). This is possibly due to its OH reaction rate-constant high enough to explain the removal of a significant toluene fraction during transport even in winter and/or toluene emissions in nearby Alpine valleys with higher mixing ratios than its background level. This example (i.e., potentially high emissions and relatively rapid removal of toluene) illustrates that the equation of factor contributions with emission source strengths can be impaired at remote sites for substances with variable reactivity or interception efficiencies. In other words, the retrieved factors might be interpreted rather as characteristic NMHC com-

positions than fresh emission profiles. Nevertheless, the average residence time of air masses in the boundary layer is estimated to be ~0.5 day (see below), whereas the atmospheric lifetime of the most labile species analyzed in this study (toluene) is five times higher. We therefore conjecture that, overall, the NMHC variability is driven by
5 source activities rather than by chemical degradation.

The three considered chlorinated NMHCs (represented in factors 2 and 4) show maxima in the warm season, highlighting their use as evaporative solvents as well as the higher impact of the industrialized Po Valley nearby on trace gas levels at Jungfraujoch during the warmer season (as mentioned in Seibert et al., 1998).

10 Correlation with gaseous tracers of primary combustion

We have hypothesized that factor 1 represents an aged combustion profile (Sect. 3.2). Indeed, its contributions are correlated with other long-lived gaseous combustion tracers such as CO and CH_4 (Table 2). The correlation of factor 1 with methane exhibits a strong seasonal dependence, ranging from rather weak (R^2=0.05...0.44) in
15 summer months (June, July, August) up to R^2=0.84...0.90 in winter months (December, January, February) – intermediate values can be calculated for months in spring (R^2=0.41...0.64) and fall (R^2=0.58...0.85). Interestingly, in spring and fall months this relationship is more adequately represented for square-root transformed factor contributions (comp. Fig. 5). In summer (low correlations), an even higher fractional contri-
20 bution of natural sources to methane can be expected compared to winter (Denman et al., 2007), e.g. caused by increased biological methanogenesis in soils or plants, which was found to be positively correlated with ambient temperature (Vigano et al., 2008). In contrast, the NMHCs defining factor 1 almost exclusively originate from anthropogenic activities. In addition, the absence of pollution events in the summery season may
25 explain this trend, but no such strong seasonality could be observed for the correlation with CO (R^2=0.40 on average), which is released predominantly by anthropogenic sources throughout the whole year (Mészáros et al., 2004).

In contrast to the first factor, factor 2 seems uncorrelated with these latter trace gases

and also with NO_x, which together with the findings in the previous chapter, indicate an industrial, non-combustive source for factor 2-species.

Potential source regions

A statistical analysis of the trajectories assigned to PMF factor contributions was per-
5   formed to deduce potential source regions of the NMHCs (comp. Sect. 2.2.3). Factor contributions (in mixing ratios, ppb) were redistributed within Europe following the approach by Stohl (1996). The resulting maps (Fig. 6) show potential source strengths in ppb and were calculated for the European continent (plus large islands), as comparatively low emissions from the sea can be expected. However, absolute mixing
10 ratios might not always be suitable to derive distinct potential source regions: clean air is transported rapidly from the Atlantic Ocean to Jungfraujoch, strongly diluting the NMHCs emitted in France. This is different for air from Eastern Europe that may be characterized by high pollution levels already when entering Europe. Thus, trajectory statistics based on absolute mixing ratios may be biased towards Eastern sources in
15 the case of Jungfraujoch. In considering this fact, maps generated with redistributed relative contributions defined by $g_{ik}/\sum_{k=1}^{4} g_{ik}$ (in % ppb/ppb) can be instructive as well and are actually shown as smaller inserts in Fig. 6 and discussed below. All trajectories assigned to NMHC measurements ($n \sim 2000$) were in contact with the planetary boundary layer for at least 20 min, but on average for 12 h. More than 90% of the assigned
20 trajectories had boundary layer contact outside Switzerland.

The sources of factor 1-species are potentially located in the Netherlands, Eastern Europe, Southern Italy, and England. These regions are in nice agreement with the spots highlighted by the EDGAR inventory for anthropogenic CH_4-emissions in Europe for the years 1997–2002 (http://www.mnp.nl/edgar/model/v32ft2000edgar/
25 edgv32ft-ghg/edgv32ft-ch4.jsp), pointing in fact to gas/oil distribution, combustion etc. or wood burning as sources related to factor 1. It is also evident that contributions from border regions of Europe are enhanced (Fig. 6). This together with the high benzene:toluene ratios (Sect. 3.1) suggests that factor 1 may not only reflect source

activity, but possibly aging as well: factor 1 presumably also reflects medium range-transport of the pollutants. High emissions from Scandinavia as well can be derived from Fig. 6, but this allocation is more uncertain: the total residence time of the back trajectories in the boundary layer of that latter region is about two magnitudes lower than for instance in Northern Italy.

Factor 2 is dominated by hydrocarbons mainly used for industrial purposes, e.g. dichloromethane as a solvent. High factor 2 contributions as well can be associated with anthropogenic emission sources located in Eastern Europe, but an additional source region is the highly industrialized Po Valley. Also Southern Spain is a candidate as a potential source region for factor 2, but given its more remote location, the trajectory statistics are more uncertain in this case (again, the total trajectory residence time per grid cell is about two magnitudes lower than e.g. in Northern Italy.)

The potential source regions for factor 3 and 4 contributions as calculated by using absolute contributions in ppb are almost identical (see Fig. 6). Factor 3 contributes the largest NMHC fraction (relative contributions, % ppb/ppb) when air masses are arriving from the South (see Fig. 6, inserted maps). This nicely corroborates the anticipated solvent-use (see Sect. 3.2) and hence temperature-dependent emissions of the relative factor contributions. Conversely, factor 4 (dominated by trichloroethene variability) contributions are most abundant when air masses are arriving from the Western sector (France/Atlantic Ocean), hinting at a distinct region of industrial sources - although potential oceanic emissions of trichloroethene have also been reported, e.g. by natural sources such as seawater algae (Dimmer et al., 2003; Abrahamsson et al., 1995; Khalil, 1999).

4 Conclusions

Four factors describing the variability of predominantly man-made NMHCs with intermediate atmospheric lifetimes (2 days to 6 months) at Jungfraujoch, Switzerland, were derived by positively constrained matrix factorization (PMF). The calculated factor con-

tributions were loaded on backward trajectories to estimate potential source regions and compared with ancillary data to infer further source information. Unique properties and source information could be associated with the estimated factors, which are not deducible by separate analyses of single compounds. The following conclusions are valid for the chosen VOC subset (non-methane hydrocarbons). The impact of various sources on total gas-phase organics (t-NMVOC) can not be inferred from the present study: clearly, sources that emit comparatively high proportions of OVOCs (e.g. biogenic sources and biomass burning; Shim et al., 2007; Gaeggeler et al., 2008) are underestimated by these analyses regarding t-NMVOC.

A factor representing highly aged fuel burning emissions accounts for 42% ppb/ppb of the mixing ratio of all 10 NMHCs considered (factor 1). It is correlated with CO (representing a tracer of anthropogenic emissions) and with CH_4, especially in wintertime when natural sources make the smallest contribution. High factor 1 activities found in winter coincided with air masses arriving from Eastern Europe, Benelux, Southern Italy and England. Interestingly, these regions overlap with the hotspots of anthropogenic methane emissions in Europe. However, the factor attributed to aged combustion (factor 1) and another hydrocarbon-dominated, but solvent-like factor (factor 3) also represent extreme benzene:toluene ratios (Fig. 1): it cannot be completely ruled out that these factors, derived for remote NMHC observations, also represent differently aged air masses. In contrast to measurements close to anthropogenic sources (Lanz et al., 2008a), this finding suggests that NMHC variability at Jungfraujoch may not only be influenced by source activities, but also by chemical processing though factors 2 and 4 cannot be associated with air mass ages (determined based on benzene:toluene ratios).

Factor 2 (28% ppb/ppb of considered NMHCs) mostly represents dichloromethane and tetrachloroethene, which are predominantly released by industrial solvent-use and production (Cox et al., 2003). Factor 2 is most active in the warm season and, furthermore, rather uncorrelated with tracers of combustive processes (CO, NO_x, and CH_4). Trajectory statistics indicate that its potential source regions are Northern Italy and (as

for all anthropogenic NMHC sources) Eastern Europe, which both harbor manufacturing industries. Relative factor contributions loaded on back trajectories provided additional information, indicating distinct source regions in the West and South for factor 3 and factor 4, respectively.

Most individual NMHCs and three out of four factors decreased from the years 2000–2001 to 2006–2007. The strengths of this decrease (in % ppb) seems somewhat related to the lifetimes of the species included in each factor, ranging from –31%. . . –38% (factors 1 and 4) to –52% (factor 3). For factor 2, on the other hand, an increase by 30% can be estimated for the same period, reflecting increasing dichloromethane and tetrachloroethene mixing ratios in recent years. The effect of European NMHC regulation policies might be overruled by increasingly higher global emissions, which is observable at Jungfraujoch only for the longest-lived substances of the considered NMHCs.

References

Abrahamsson, K., Ekdahl, A., Collén, J., and Pedersén, M.: Marine algae – A source of trichloroethylene and perchloroethylene, Limnol. Oceanogr., 40, 1321–1326, 1996.

Atkinson, R. and Arey, J.: Atmospheric degradation of volatile organic compounds, Chem. Rev., 103, 4605–4638, 2003.

Carpenter, L. J., Green, T. J., Mills, G. P., Bauguitte, S., Penkett, S. A., Zanis, P., Schuepbach, E., Schmidbauer, N., Monks, P. S., and Zellweger, C.: Oxidized nitrogen and ozone production efficiencies in the springtime free troposphere over the Alps, J. Geophys. Res., 105(D11), 14 547–14 559, 2000.

Cox, M. L., Sturrock, G. A., Fraser, P. J., Siems, S. T., Krummel, P. B., and O'Doherty, S.: Regional sources of methyl chloride, chloroform and dichloromethane identified from AGAGE observations at Cape Grim, Tasmania, 1998–2000, J. Atmos. Chem., 45, 79–99, 2003.

Cozic, J., Verheggen, B., Weingartner, E., Crosier, J., Bower, J. N., Flynn, M., Coe, H., Henning, S., Steinbacher, M., Henne, S., Coen, M. C., Petzold, A., and Baltensperger, U.: Chemical composition of free tropospheric aerosol for PM_1 and coarse mode at the high alpine site Jungfraujoch, Atmos. Chem. Phys., 8, 407–423, 2008,
http://www.atmos-chem-phys.net/8/407/2008/.

Denman, K. L., Brasseur, G., Chidthaisong, A., Ciais, P., Cox, P. M., Dickinson, R. E., Hauglustaine, D., Heinze, C., Holland, E., Jacob, D., Lohmann, U., Ramachandran, S., da Silva Dias, P. L., Wofsy, S. C., and Zhang, X.: Couplings Between Changes in the Climate System and Biogeochemistry. in: Climate Change 2007: The Physical Science Basis. Contribution of Working Group I to the Fourth Assessment Report of the Intergovernmental Panel on Climate Change, edited by: Solomon, S., Qin, D., Manning, M., Chen, Z., Marquis, M., Averyt, K. B., Tignor, M., and Miller, H. L., Cambridge University Press, Cambridge, UK and New York, NY, USA, 2007.

Dimmer, C. H., McCulloch, A., Simmonds, P. G., Nickless, G., Bassford, M. R., and Smythe-Wright, D.: Tropospheric concentrations of the chlorinated solvents, tetrachloroethene and trichloroethene, measured in the remote Northern Hemisphere, Atmos. Environ., 35, 1171–1182, 2001.

Fay, B., Glaab, H., Jacobsen, I., and Schrodin, R.: Evaluation of Eulerian and Lagrangian atmosphere transport models at Deutscher Wetterdienst using ANATEX surface tracer data, Atmos. Environ., 29, 2485–2497, 1995.

Forrer, J., Rüttimann, R., Scheiter, D., Fischer, A., Buchmann, B., and Hofer, P.: Variability of trace gases at the high-Alpine site Jungfraujoch by meteorological transport processes, J. Geophys. Res., 105(D10), 12 241–12 251, 2000.

Gaeggeler, K., Prévôt, A. S. H., Dommen, J., Legreid, G., Reimann, S., and Baltensperger, U: Residential wood burning in an Alpine valley as a source for oxygenated volatile organic compounds, hydrocarbons and organic acids, Atmos. Environ., doi:10.1016/j.atmosenv.2008.07.038), in press, 2008

Golub, G. H. and Van Loan, C. F.: Matrix Computations (Third Edition), The Johns Hopkins University Press, Baltimore, MD, USA, 1996.

Henne, S., Furger, M., and Prévôt, A. S. H.: Climatology of mountain venting-induced elevated

moisture layers in the lee of the Alps, J. Appl. Meteorol., 44, 620–633, 2005.

Henne, S., Junkermann, W., Kariuki, J. M., Aseyo, J., and Klausen, J.: The establishment of the Mt. Kenya GAW station: installation and meteorological characterization, J. Appl. Meteorol. Clim., accepted, 2008a.

5 Henne, S., Klausen, J., Junkermann, W., Kariuki, J. M., Aseyo, J. O., and Buchmann, B.: Representativeness and climatology of carbon monoxide and ozone at the global GAW station Mt. Kenya in equatorial Africa, Atmos. Chem. Phys., 8, 3119–3139, 2008b, http://www.atmos-chem-phys.net/8/3119/2008/.

Henry, R. C.: History and fundamentals of multivariate air quality receptor models, Chemometr.
10 Intell. Lab., 37, 37–42, 1997.

Henry, R. C.: Multivariate receptor modelling by N-dimensional edge detection, Chemometr. Intell. Lab., 65, 179–189, 2003.

Keene, W. C., Khalil, M. A. K., Erickson, D. J., McCulloch, A., Graedel, T. E., Lobert, J. M., Aucott, M. L., Gong, S. L., Harper, D. B., Kleiman, G., Midgley, P., Moore, R. M., Seuzaret, C.,
15 Sturges, W. T., Benkovitz, C. M., Koropalov, V., Barrie, L. A., and Li, Y. F.: Composite global emissions of reactive chlorine from anthropogenic and natural sources: Reactive Chlorine Emissions Inventory, J. Geophys. Res., 104(D7), 8429–8440, 1999.

Khalil, M. A. K.: Reactive chlorine compounds in the atmosphere, in: Reactive Halogen Compounds in the Atmosphere, edited by: Fabian, P. and Singh, O. N., 45-79, Springer, New
20 York, USA, 1999.

Kleiman, G. and Prinn, R. G.: Measurement and deduction of emissions of trichloroethene, tetrachloroethene, and trichloromethane (chloroform) in the northeastern United States and southeastern Canada, J. Geophys. Res., 105(D23), 28 875–28 893, 2000.

Klemp, D., Kley, D., Kramp, F., Buers, H. J., Pilwat, G., Flocke, F., Pätz, H. W., and Volz-Thomas,
25 A.: Long-Term Measurements of Light Hydrocarbons (C_2–C_5) at Schauinsland (Black Forest), J. Atmos. Chem., 28, 135–171, 1997.

Ko, M. K. W. and Poulet, G.: Very short-lived halogens and sulfur substances, in Scientific Assessment of Ozone Depletion: 2002, Global Ozone Res. and Monit. Proj. Rep., 47, chap. 2, 2.1–2.57, World Meteorol. Organ., Geneva, Switzerland, 2003.

30 Krzanowski, W. J.: Principles of multivariate analysis: a user's perspective, Clanderon Press, Oxford, UK, 1988.

Lanz, V. A., Alfarra, M. R., Baltensperger, U., Buchmann, B., Hueglin, C., and Prévôt, A. S. H.: Source apportionment of submicron organic aerosols at an urban site by factor analytical

modelling of aerosol mass spectra, Atmos. Chem. Phys., 7, 1503–1522, 2007,
http://www.atmos-chem-phys.net/7/1503/2007/.

Lanz, V. A., Hueglin, C., Buchmann, B., Hill, M., Locher, R., Staehelin, J., and Reimann, S.: Receptor modeling of C_2-C_7 hydrocarbon sources at an urban background site in Zurich, Switzerland: changes between 1993-1994 and 2005-2006, Atmos. Chem. Phys., 8, 2313–2332, 2008a,
http://www.atmos-chem-phys.net/8/2313/2008/.

Lanz, V. A., Alfarra, M. R., Baltensperger, U., Buchmann, B., Hueglin, C., Szidat, S., Wehrli, M. N., Wacker, L., Weimer, S., Caseiro, A., Puxbaum, H., and Prévôt, A. S. H.: Source attribution of submicron organic aerosols during wintertime inversions by advanced factor analysis of aerosol mass spectra, Environ. Sci. Technol., 42, 214–220, 2008b.

Legreid, G., Folini, D., Staehelin, J., Balzani Lööv, J., Steinbacher, M., and Reimann, S.: Measurements of organic trace gases including oxygenated volatile organic compounds at the high alpine site Jungfraujoch (Switzerland): Seasonal variation and source alloctaion, J. Geophys. Res., 113, D05307, doi:10.1029/2007JD00863, 2008.

Li, Y., Campana, M., Reimann, S., Schaub, D., Stemmler, K., Staehelin, J., and Peter, T.: Hydrocarbon concentrations at the Alpine mountain sites Jungfraujoch and Arosa, Atmos. Environm., 39, 1113–1127, 2005.

Lugauer, M., Baltensperger, U., Furger, M., Gaeggeler, H. W., Jost, D. T., Schwikowski, M., and Wanner, H.: Aerosol transport to the high Alpine sites Jungfraujoch (3453 m a.s.l.) and Colle Gnifetti (4452 m a.s.l.), Tellus, 50B, 76–92, 1998.

McCulloch, A. and Midgley, P. M.: The production and global distribution of emissions of trichloroethene, tetrachloroethene and dichloromethane over the period 1988–1992, Atmos. Environ., 30, 601–608, 1996.

McKeen, S. A. and Liu, S. C.: Hydrocarbon ratios and photochemical history of air masses, Geophys. Res. Lett., 20, 2363–2366, 1993.

Mészáros, T., Haszpra, L., and Gelencsér, A.: The assessment of the seasonal contribution of the anthropogenic sources to the carbon monoxide budget in Europe, Atmos. Environ., 38, 4147–4154, 2004.

Monks, P. S.: A review of the observations and origins of the spring ozone maximum, Atmos. Environ., 34, 3545–3561, 2000.

Novelli, P. C., et al.: An internally consistent set of globally distributed atmospheric carbon monoxide mixing ratios developed using results from an intercomparison of measurements,

Factor analysis of remote NMHCs

V. A. Lanz et al.

Title Page

Abstract	Introduction
Conclusions	References
Tables	Figures

|◄ | ►|

◄ | ►

Back | Close

Full Screen / Esc

Printer-friendly Version

Interactive Discussion

J. Geophys. Res., 103(D15), 19 285–19 293, 1998.

Ordóñez, C., Brunner, D., Staehelin, J., Hadjinicolaou, P., Pyle, J. A., Jonas, M., Wernli, H., and Prévôt, A. S. H.: Strong influence of lowermost stratospheric ozone on lower free tropospheric ozone changes over Europe, Geophys. Res. Lett., 34, L07805, doi:10.1029/2006GL029113, 2007.

Paatero, P.: Least squares formulation of robust non-negative factor analysis, Chemometr. Intell. Lab., 37, 23–35, 1997.

Paatero, P. and Tapper, U.: Analysis of different modes of factor-analysis as least-squares fit problems, Chemometr. Intell. Lab., 8, 183–194, 1993.

Paatero, P. and Tapper, U.: Positive matrix factorization: a nonnegative factor model with optimal utilization of error estimates of data values, Environmetrics, 5, 111–126, 1994.

Reimann, S., Schaub, D., Stemmler, K., Folini, D., Hill, M., Hofer, P., Buchmann, B. and Simmonds, P. G. and Greally, B. R., and O'Doherty, S.: Halogenated greenhouse gases at the Swiss High Alpine Site of Jungfraujoch (3580 m a.s.l.): Continuous measurements and their use for regional European source allocation, J. Geophys. Res., 109, D5, doi:10.1029/2003JD003923, 2004.

Reimann, S., Manning, A. J., Simmonds, P. G., Cunnold, D. M., Wang, R. H., Li, J. L., McCulloch, A., Prinn, R. G., Huang, J., Weiss, R. F., Fraser, P. J., O'Doherty, S., Greally, B. R., Stemmler, K., Hill, M., and Folini, D.: Low European methyl chloroform emissions inferred from long-term atmospheric measurements, Nature, 433, 506–508, 2005.

Reimann, S., Vollmer, M. K., Folini, D., Steinbacher, M., Hill, M., Buchmann, B., Zander, R., and Mahieu, E.: Longterm observations of anthropogenic halocarbons at the high-alpine site of Jungfraujoch (Switzerland) for assessment of trends and European sources , Sci. Total Env., 391, 224–231, 2008.

Roberts, J. M., Fehsenfeld, F. C., Liu, S. C., Bollinger, M. J., Hahn, C., Albritton, D. L., and Sievers, R. E.: Measurements of aromatic hydrocarbon ratios and NO$_x$ concentration in the rural troposphere: Observation of air mass photochemical aging and NO$_x$ removal, Atmos. Environ., 18, 2421–2432, 1984.

Saarikoski, S., Timonen, H., Saarnio, K., Aurela, M., Järvi, L., Keronen, P., Kerminen, V.-M., and Hillamo, R.: Sources of organic carbon in fine particulate matter in northern European urban air, Atmos. Chem. Phys., 8, 6281–6295, 2008, http://www.atmos-chem-phys.net/8/6281/2008/.

Sandradewi, J., Prévôt, A. S. H., Szidat, S., Perron, N., Alfarra, M. R., Lanz, V. A., Weingartner,

Title Page

Abstract | Introduction

Conclusions | References

Tables | Figures

◄ | ►

◄ | ►

Back | Close

Full Screen / Esc

Printer-friendly Version

Interactive Discussion

E., and Baltensperger, U.: Using aerosol light absorption measurements for the quantitative determination of wood burning and traffic emission contributions to particulate matter, Environ. Sci. Technol., 42, 3316–3323, 2008.

Seber, G. A. F.: Multivariate observations, Wiley, New York, USA, 1984.

5 Seibert, P., Kromp-Kolb, H., Baltensperger, U., et al.: In Transport and Transformation of Pollutants in the Troposphere, Academic Publishing, Den Haag, The Netherlands, 689–693,1994.

Seibert, P., Kromp-Kolb, H., Kasper, A., Kalina, M., Puxbaum, H., Jost, D. T., Schwikowski, M., and Baltensperger, U.: Transport of polluted boundary layer air from the Po Valley to high-alpine sites, Atmos. Environ., 32, 3953–3965, 1998.

10 Shim, C., Wang, Y., Singh, H. B., Blake, D. R., and Guenther, A. B.: Source characteristics of oxygenated volatile organic compounds and hydrogen cyanide, J. Geophys. Res., 112, D10305, doi:10.1029/2006JD007543, 2007.

Simmonds, P. G., O'Doherty, S., Nickless, G., Sturrock, G. A., Swaby, R., Knight, P., Ricketts, J., Woffendin, G., and Smith, R.: Automated gas chromatograph mass spectrometer for routine

15 atmospheric field measurements of the CFC replacement compounds, the hydrofluorocarbons and hydrochlorofluorocarbons, Anal. Chem., 67, 717–723, 1995.

Simmonds, P. G., Manning, A. J., Cunnold, D. M., et al.: Global trends, seasonal cycles, and European emissions of dichloromethane, trichloroethene, and tetrachloroethene from the AGAGE observations at Mace Head, Ireland, and Cape Grim, Tasmania, J. Geophys. Res.,

20 111, D18304, doi:10.1029/2006JD007082, 2006.

Stohl, A.: Trajectory statistics – a new method to establish source-receptor relationships of air pollutants and its application to the transport of particulate sulfate in Europe, Atmos. Environ., 30, 579–587, 1996.

Thoning, K. W., Tans, P. P., and Komhyr, W. D.: Atmospheric carbon dioxide at Mauna Loa

25 Observatory 2. Analysis of the NOAA GMCC Data, 1974–1985, J. Geophys. Res., 94(D6), 8549–8565, 1989.

Vigano, I., van Weelden, H., Holzinger, R., Keppler, F., McLeod, A., and Röckmann, T.: Effect of UV radiation and temperature on the emission of methane from plant biomass and structural components, Biogeosci., 5, 937–947, 2008.

30 Walker, S. J., Evans, M. J., Jackson, A. V., Steinbacher, M., Zellweger, C., and McQuaid, J. B.: Processes controlling the concentration of hydroperoxides at Jungfraujoch Observatory, Switzerland, Atmos. Chem. Phys., 6, 5525–5536, 2006, http://www.atmos-chem-phys.net/6/5525/2006/.

Zanis, P., Monks, P. S., Green, T. J., Schuepbach, E., Carpenter, L. J., Mills, G. P., Rickard, A. R., Brough, N., and Penkett, S. A.: Seasonal variation of peroxy radicals in the lower free troposphere based on observations from the FREE Tropospheric EXperiments in the Swiss Alps, Geophys. Res. Lett., 30(10), 1497, doi:10.1029/2003GL017122, 2003.

5 Zanis, P., Ganser, A., Zellweger, C., Henne, S., Steinbacher, M., and Staehelin, J.: Seasonal variability of measured ozone production Efficiencies in the lower free troposphere of Central Europe, Atmos. Chem. Phys., 7, 223–236, 2007,
http://www.atmos-chem-phys.net/7/223/2007/.

Zellweger, C., Ammann, M., Buchmann, B., Hofer, P., Lugauer, M., Rüttimann, R., Streit, N.,
10 Weingartner, E., and Baltensperger, U.: Summertime NO_y speciation at the Jungfraujoch, 3580 m above sea level, Switzerland, J. Geophys. Res., 105 (D5), 6655–6667, 2003.

Zellweger, C., Forrer, J., Hofer, P., Nyeki, S., Schwarzenbach, B., Weingartner, E., Ammann, M., and Baltensperger, U.: Partitioning of reactive nitrogen (NOy) and dependence on meteorological conditions in the lower free troposphere, Atmos. Chem. Phys., 3, 779–796, 2003,
15 http://www.atmos-chem-phys.net/3/779/2003/.

Table 1. Mean mixing ratios, $\overline{x_j}$, standard deviations, sd(x_j), in ppt of the 10 considered NMHC species for the years 2000–2008 ($n \sim 60\,000$), and their estimated lifetimes in the atmosphere as calculated from Arey and Atkinson (2003) (hydrocarbons) or derived from McCulloch and Midgley (1996), Kleiman and Prinn (2000), and Ko and Poulet (2003) (chlorinated NMHCs).

species j	synonym	formula	$\overline{x_j}$ [ppt]	sd(x_j) [ppt]	lifetime
isobutane	2-methylpropane	C_4H_{10}	62	59	7 d
butane	n-butane	C_4H_{10}	97	114	6 d
isopentane	2-methylbutane	C_5H_{12}	61	68	3 d
pentane	n-pentane	C_5H_{12}	29	35	4 d
dichloromethane	methylene chloride, DCM	CH_2Cl_2	42	22	5–6 mo
hexane	n-hexane	C_6H_{14}	11	15	3 d
benzene	benzol	C_6H_6	51	46	12 d
trichloroethene	trichlorethylene, TCE	C_2HCl_3	4	6	5–11 d
toluene	methylbenzene	C_7H_8	46	76	2 d
tetrachloroethene	perchlorethylene, PCE	C_2Cl_4	8	8	3–7 mo

Table 2. Coefficients of determination (R^2) for linear regressions of factor contributions vs. ancillary tracers for combustion (CO, NO_x, CH_4): $[tracer]_i = a_k g_{ik} + b_k$. Estimates for a_k are all significantly different from 0 on the $p<0.05$ level. Non-zero intercepts ($b_k > 0$) can be calculated for regression models involving CO (b_k=0.10...0.12 ppm) and CH_4 (b_k=1.82...1.84 ppm). $R^2 \geq 0.50$ in **bold**, $R^2 \geq 0.40$ in *italics*. (n: number of observations.)

R^2 (n)	CO (8983)	NO_x (7202)	CH_4 (2720)
factor 1	*0.40*	0.24	**0.50**
factor 2	0.17	0.14	0.26
factor 3	0.22	*0.43*	0.22
factor 4	0.22	0.36	0.20

Table 3. Mean source contributions estimates (SCE), mean($g_{ik}/\sum_j x_{ij}$), and the standard deviation of the mean in brackets. Seasonal abundance of the contribution as absolute values (ppb) and percentages (%) (s: summer source, w: winter source). Potential source regions (PSR) in Europe as calculated by trajectory statistics for absolute (ppb) and relative (%) factor contributions (N: North, S: South, E: East, W: West). Key species in each factor as defined by an explained variation (EV_{kj}) >50% (concept of EV_{kj} see Sect. 3.2). A tentative interpretation of the PMF factors as NMHC sources is given as well.

factor k	SCE (%)	season (ppb)	season (%)	correlation	PSR (ppb)	PSR (%)	key species	interpretation
$k=1$	42 (0.2)	w	w	CH_4, (CO)	NE	NE	(iso-)butane	aged, combustion
$k=2$	28 (0.2)	s	s	–	SE	NSEW	CH_2Cl_2, C_2Cl_4	industrial, non-combustion
$k=3$	19 (0.1)	–	s	(NO_x)	SE	S	toluene	fresh, solvent-use
$k=4$	5 (0.1)	–	s	–	SE	W	C_2HCl_3	industrial, non-combustion
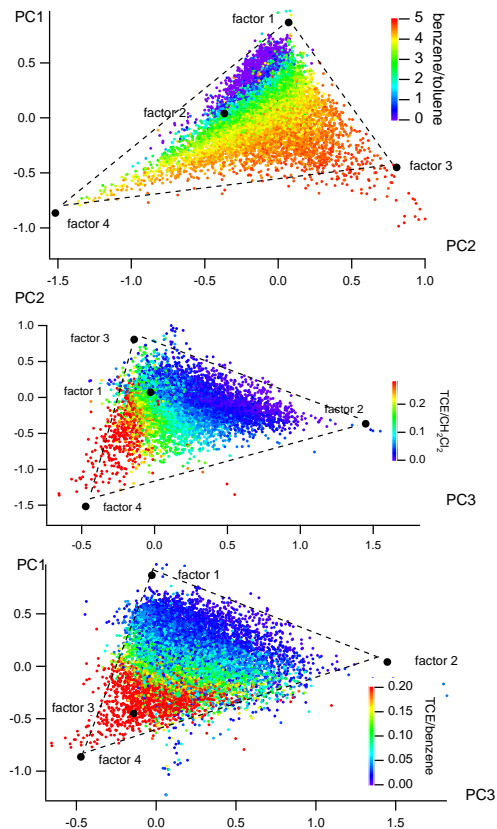
Fig. 1. Data samples ($n\sim 10000$) and PMF-resolved profiles ($p=4$) projected onto the standardized PC planes (PC: principal components). The ratio benzene/toluene is shown for samples in the PC1 vs. PC2 plane (top), the ratio TCE/CH_2Cl_2 for PC2 vs. PC3 (middle), and the TCE/benzene-ratio for PC1 vs. PC3 (down) (TCE: trichloroethene).
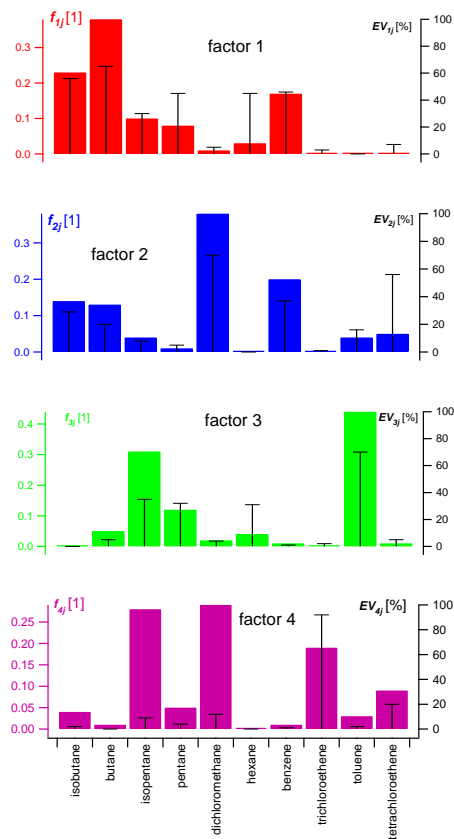
Fig. 2. Factor profiles as calculated by PMF. The factor profiles sum to unity, $f_{kj}[1] := \sum_j f_{kj} = 1$, and are indicated by the colored bars (left axis). The variability of each compound that is explained by the kth factor, EV [%], is shown on the right axis (whiskers).

Printer-friendly Version

Interactive Discussion

Printer-friendly Version

Interactive Discussion
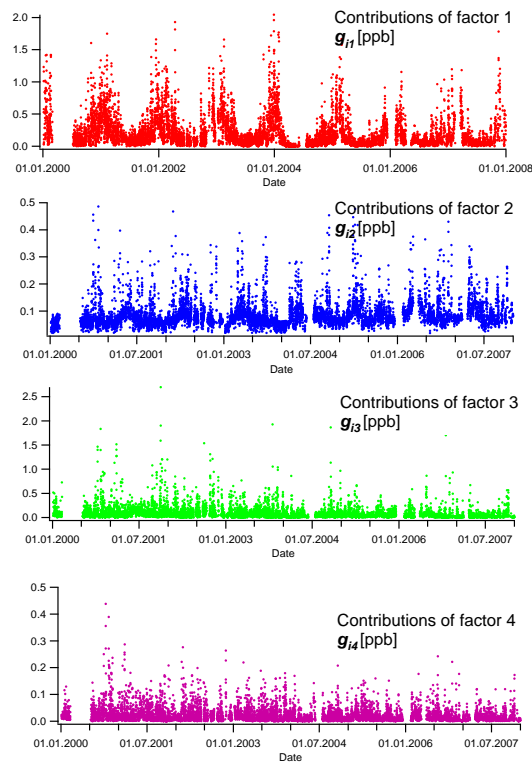
Fig. 3. Time series of the factor contributions as mixing ratios ppb (derived from NMHC measurements at Jungfraujoch during 2000-2007; $n \sim 10000$)
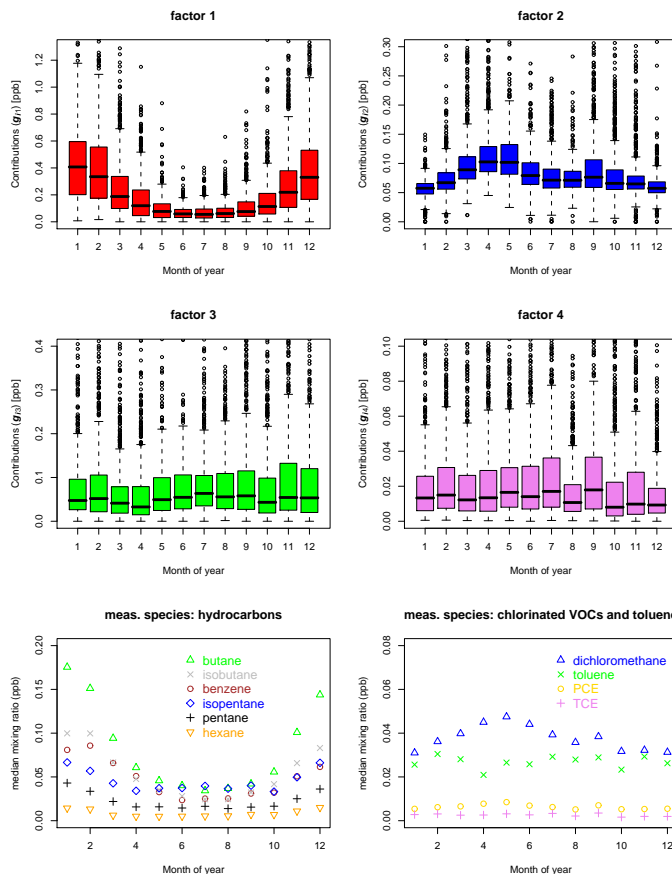
Fig. 4. Monthly boxplots of the four PMF factor contributions in ppb ($n\sim10000$). The horizontal bar represents the median, the boxes are confined by the 1st and 3rd quartile. Circles represent extreme observations. Monthly median values are shown for the observed in-situ measurements of the 10 NMHCs considered (down). (TCE: trichloroethene, PCE: tetrachloroethene.)

◄   ►

◄   ►

Back   Close

Full Screen / Esc

Printer-friendly Version

Interactive Discussion
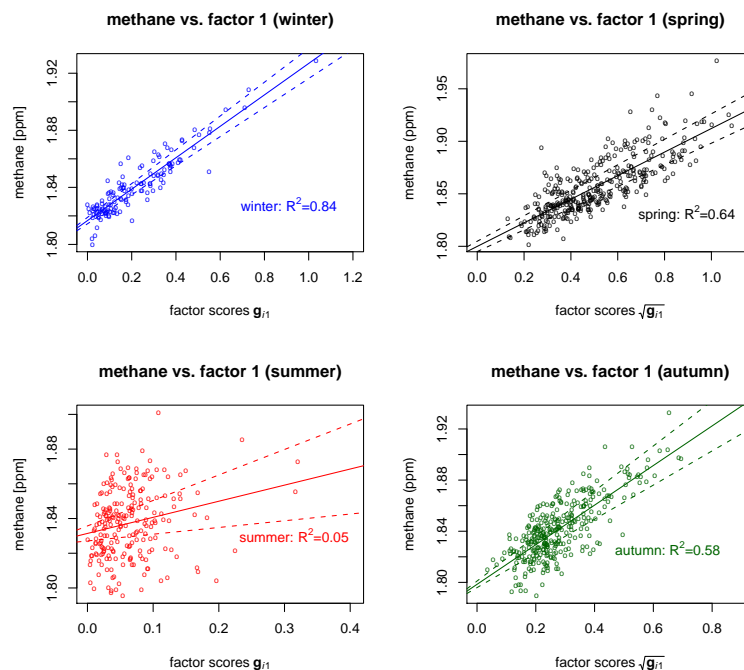
Fig. 5. Scatter plots for methane vs. factor 1: linear regression slopes, intercept, and R^2 indicated for winter, spring, summer, and autumn represented by December (n=132), March (n=346), June (n=223), and September (n=324), respectively. For spring and fall months, a square root-transformation of the scores clearly reduces the interdependence of the residuals of the linear regression model and typically increases R^2. Dashed lines represent the 2σ uncertainties of slopes and intercepts.
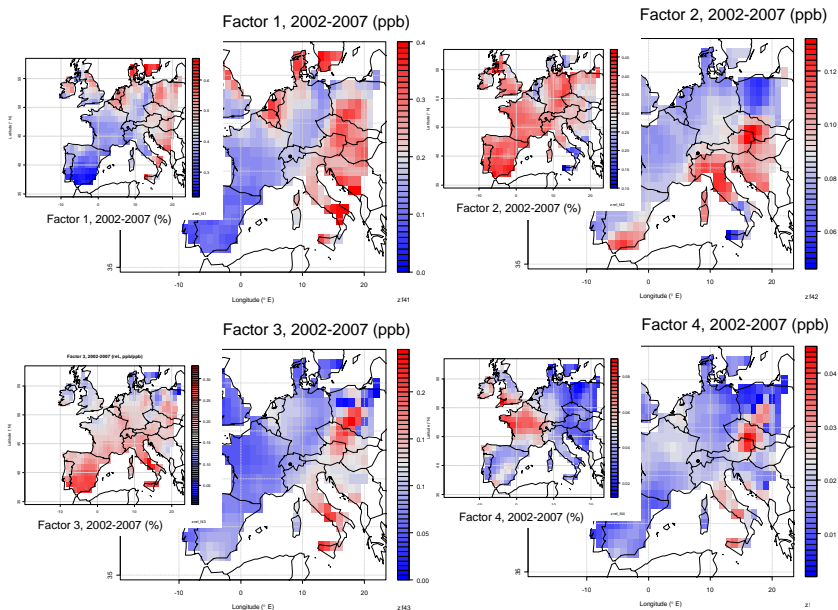
Fig. 6. Trajectory statistics calculated for the contributions (ppb) of four factors. Back trajectories were calculated based on COSMO weather forecasts (2 days). The inserted figures show the trajectory statistics for the relative source strengths (%) of the factors. $n \sim 2000$